Malignant Neoplasm

11

Yoshinobu Maeda, Akihiko Kawahara, Takeshi Nishikawa, and Yoshiaki Norimatsu

11.1 Endometrial Endometrioid Carcinoma

11.1.1 Background

Endometrial endometrioid carcinoma (EEC) is the most common histological type of endomerial carcinoma (EC), accounting for more than 75% of all endometrial carcinomas. The incidence of endometrial carcinomas varies globally, with age-standardized incidence rates varying from 1 to 25 cases per 100,000 person-years in 2018. In Japan, the incidence of endometrial carcinomas has steadily increased in recent years.

The median patient age at the onset of EEC was 63 years [1]. It is well known that irregular genital bleeding is observed in postmenopausal women. The highest incidence rates occur in North America and Europe. The lowest incidence rate (4–5 times lower) is found in countries with low human development index [1, 2].

A major cause of the development of EEC is prolonged exposure to unopposed estrogen stimulation associated with an ovulation disorder such as polycystic ovarian syndrome, estrogen replacement therapy, tamoxifen treatment for breast cancer, and estrogen-producing neoplasms (e.g., ovarian thecoma and granulosa cell tumor.)

Y. Maeda
Department of Diagnostic Pathology, Toyama Red Cross Hospital, Toyama, Japan

A. Kawahara
Department of Diagnostic Cytopathology, Kurume University Hospital, Fukuoka, Japan

T. Nishikawa
Department of Diagnostic Pathology, Nara Medical University Hospital, Kashihara, Nara, Japan

Y. Norimatsu (✉)
Department of Medical Technology, Faculty of Health Sciences, Ehime Prefectural University of Health Sciences, Tobe-cho, Iyo-gun, Ehime, Japan
e-mail: ynorimatsu@epu.ac.jp

Y. Hirai, F. Fulciniti (eds.), *The Yokohama System for Reporting Endometrial Cytology*, https://doi.org/10.1007/978-981-16-5011-6_11

Early menarche, late menopause, nulliparity, obesity, and diabetes are well-known risk factors for EEC. In addition to these factors, Lynch syndrome with a mutation in DNA mismatch repair genes and Cowden syndrome caused by *PTEN* mutation are associated with familial endometrioid carcinoma [1, 2].

In the 1980s, ECs were classified as estrogen-dependent type I or estrogen-independent type II tumors by Bokhman [3]. Representative subtypes of type I are approximately corresponding to EECs, grade1 (G1) and grade2 (G2), which develop from endometrial atypical hyperplasia/endometrioid intraepithelial neoplasia (EIN). On the other hand, EEC, grade3 (G3) is classified as type II, which arises de novo from atrophic endometrium [2, 4].

In 2013, The Cancer Genome Atlas (TCGA) study divided endometrioid carcinoma into four subgroups, integrating genomic profiles, such as "ultramutated," "hypermutated," "copy number low," and "copy number high." [5]

11.1.2 Definition

EEC is a malignant epithelial neoplasm displaying varying proportions of glandular, papillary, and solid architecture, with neoplastic cells showing endometrioid differentiation. These tumors are referred to as "endometrioid" due to their similarity to proliferative phase endometrium [1, 2].

EEC is typically composed of columnar cells with eosinophilic and granular cytoplasm and has a low account of mucin. Histologically the tumor displays glandular, papillary with fine fibrovascular stroma, and solid pattern (Fig. 11.1). Nuclear

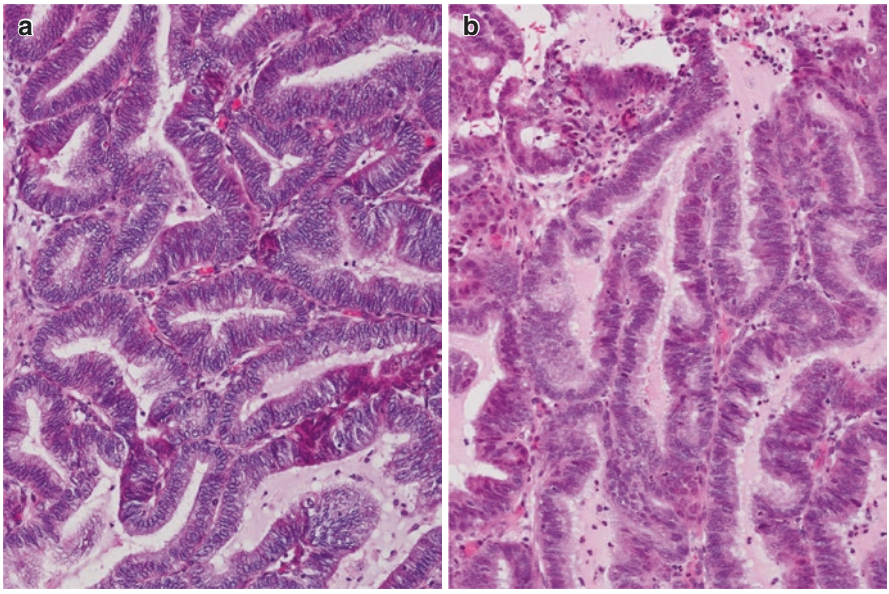

Fig. 11.1 EEC, G1. Histologic preparation shows irregularly shaped glands (**a**) and papillary architecture (**b**). (HE stain, original magnification **a** and **b**: 20x)

pseudostratification is usually observed and nuclear atypia is mild to moderate. Nucleoli are mostly inconspicuous [1, 2].

EECs were divided into three grades (G1, G2 or G3) according to the FIGO grading criteria. They are based on histological architecture and cellular atypia.

The architectural grade was determined according to the presence of a solid component without squamous differentiation. EEC, G1; the proportion of solid components is no more than 5%. EEC, G2; the proportion of solid growth is 6–50%, and EEC, G3; the glandular structure remains irregularly in some areas but is extremely obscured, and more than half is composed of the solid component.

Alternatively, if the rate of solid component is less than 5% and 6–50%, but the cell atypia is remarkable, raise G2, G3 instead of G1, G2, respectively [1, 2].

EECs have some histological and cytological variants. Squamous differentiation is composed of keratinizing cells and/or eosinophilic cells, including as morules occurring in 10–25% of endometrioid carcinomas. Other histological patterns include a secretory pattern in which the majority of tumor cells resemble early secretory phase endometrial glands, ciliated pattern, microglandular pattern, spindle cell pattern, sertoliform pattern, and mucinous pattern in various proportions in tumors [1, 2].

11.1.3 Cytologic Diagnostic Criteria [6–10] (Figs. 11.2, 11.3, 11.4, 11.5, 11.6, 11.7, 11.8 and 11.9)

- Almost all clusters show an irregular protrusion pattern.
- The nuclear overlap in epithelial cell clusters exceeds three layers, and the cohesion of stroma cells around the clusters is absent.
- Usually, epithelial cell clusters show glandular complexity with an increasing number of lumens, observed as a cribriform pattern in histologic preparation.

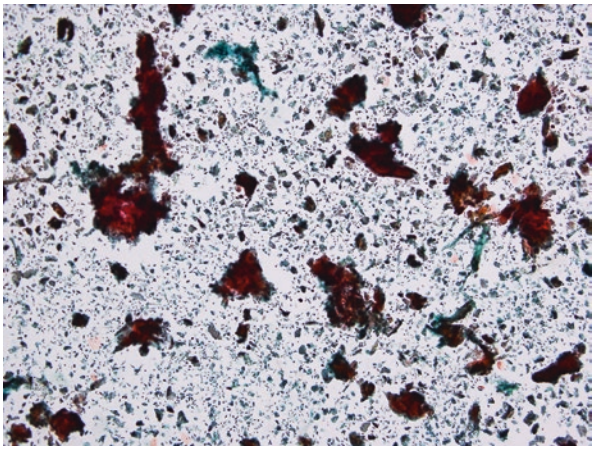

Fig. 11.2 EEC, G1. Same sample as Fig. 11.1. This cytological preparation was obtained from a 40 y-o woman with irregular genital bleeding. Many clusters show various sizes and irregular shapes. (Papanicolaou stain, original magnification 4×)

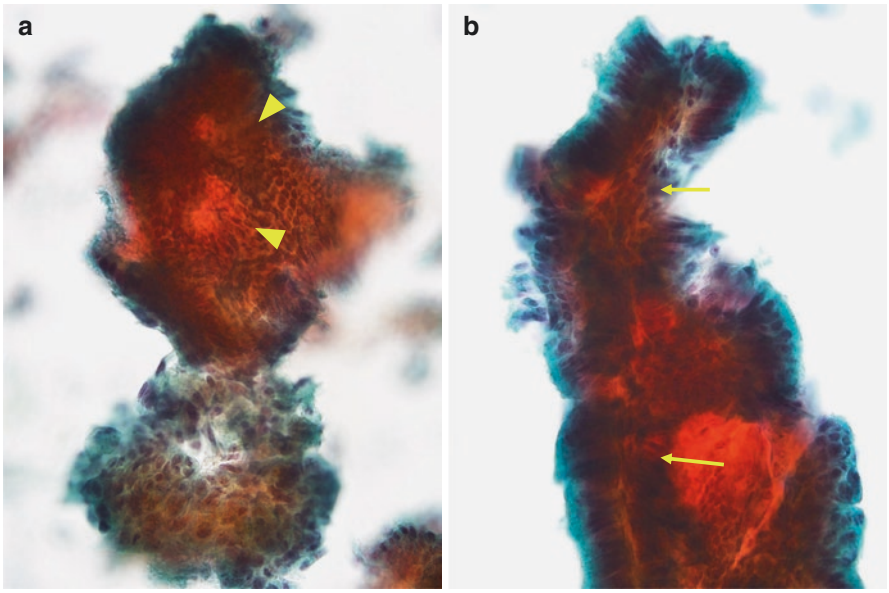

Fig. 11.3 EEC, G1. Same sample as Fig. 11.1. (**a**): An irregularly shaped cluster with lumens (arrowheads) is seen. (**b**): Fine strands consisted spindle cells (arrows) are seen in cellular clusters and nuclei of tumor cells are arranged perpendicular to strands. (Papanicolaou stain, original magnification **a** and **b**: 40×)

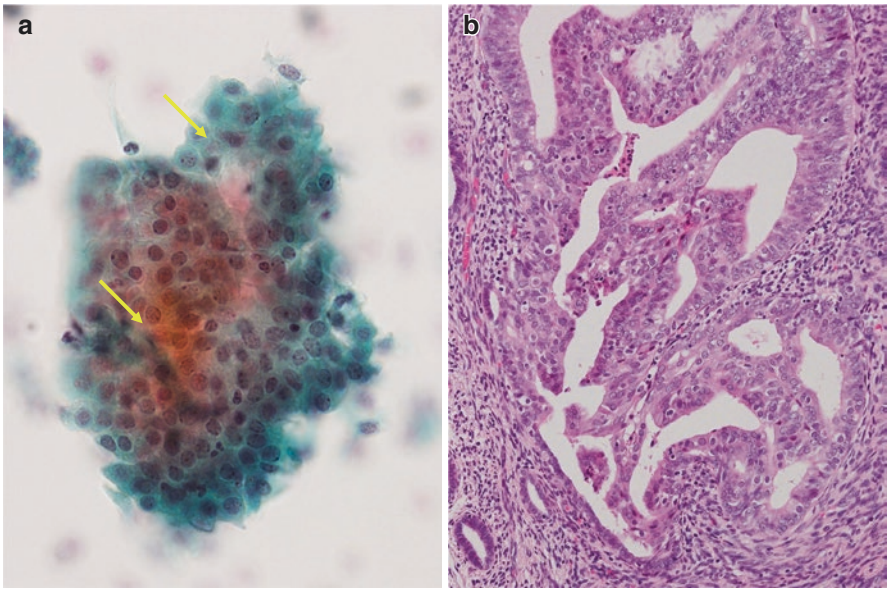

Fig. 11.4 EEC, G1. An irregularly shaped cluster with lumens (arrows) and nuclear overlapping is seen. Nuclei are enlarged, have conspicuous nucleoli. (**a**) Corresponding to histologic preparation (**b**), dilated and irregular shaped glands are present. (**a**: Papanicolaou stain, original magnification 60×, **b**: HE stain, original magnification 20×)

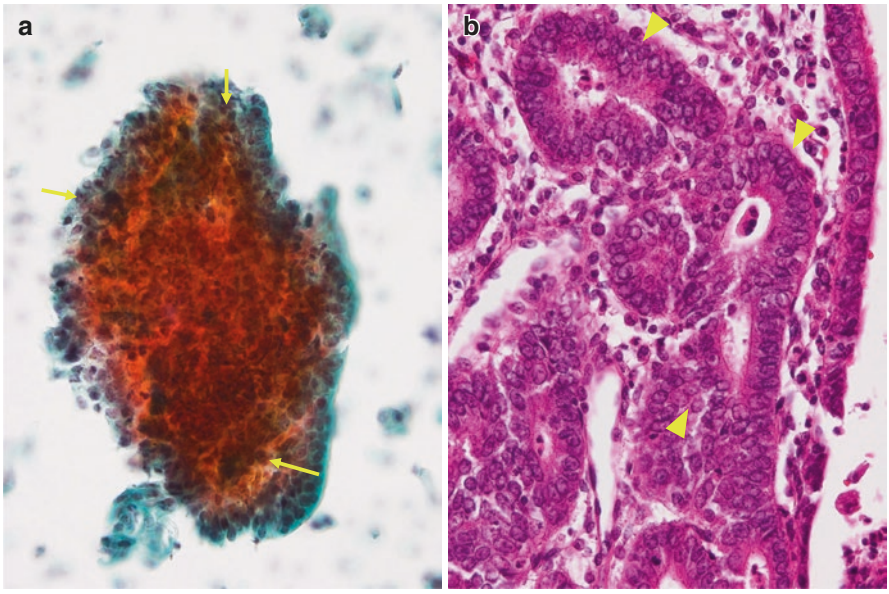

Fig. 11.5 EEC, G1. Irregularly shaped lumens (arrows) increase numbers in cellular clusters. (**a**) Corresponding to histologic preparation (**b**), irregular shaped fused glands are present (arrowheads). (**a**: Papanicolaou stain, original magnification 40×, **b**: HE stain, original magnification 40×)

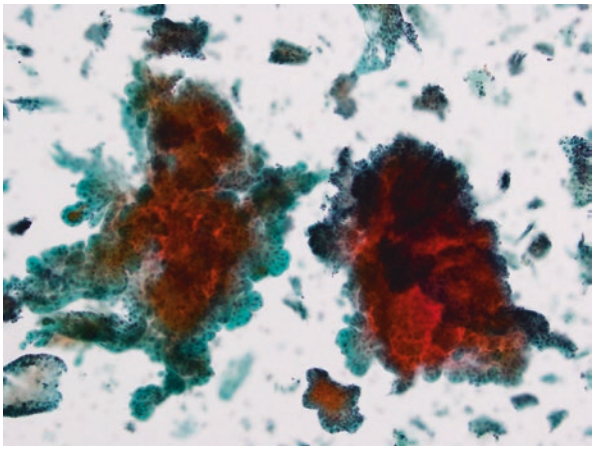

Fig. 11.6 EEC, G1, with squamous differentiation. Large and irregular clusters can be seen. (Papanicolaou stain, original magnification 10×)

- The arrangement in the epithelial cell clusters becomes irregular, and the nucleus frequently protrudes toward the periphery of the clusters.
- Glandular epithelial cells with nuclear swelling, anisonucleosis, increased chromatin granularity, and conspicuous nucleoli are observed.
- Mitosis can be occasionally observed.
- Hemorrhagic and necrotic exudate can be seen in the background.

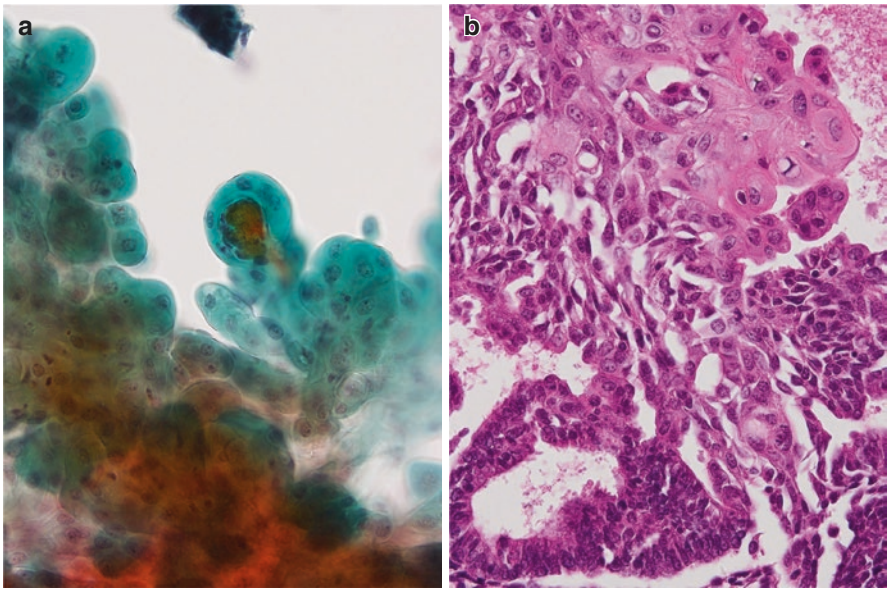

Fig. 11.7 EEC, G1, with squamous differentiation. (**a**): Tumor cells with light-green cytoplasm show a low N/C ratio, and nuclei are located centrally. (**b**): Corresponding to histologic preparation shows squamous differentiation with single-cell keratinization (upper right). (**a**: Papanicolaou stain, original magnification 40×, **b**: HE stain, original magnification 40×)

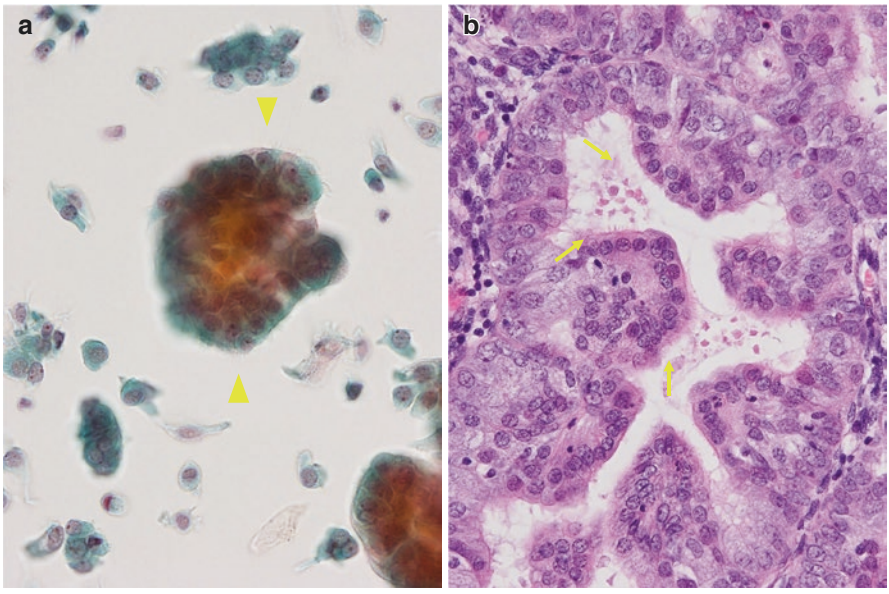

Fig. 11.8 EEC, G1, with ciliated change. Neoplastic epithelial cells (**a**) with cilia are intermingled in cellular clusters (arrowheads). Corresponding to histologic preparation (**b**), ciliated neoplastic cells are seen along luminal aspect (arrows). (**a**: Papanicolaou stain, original magnification 60×, **b**: HE stain, original magnification 40×)

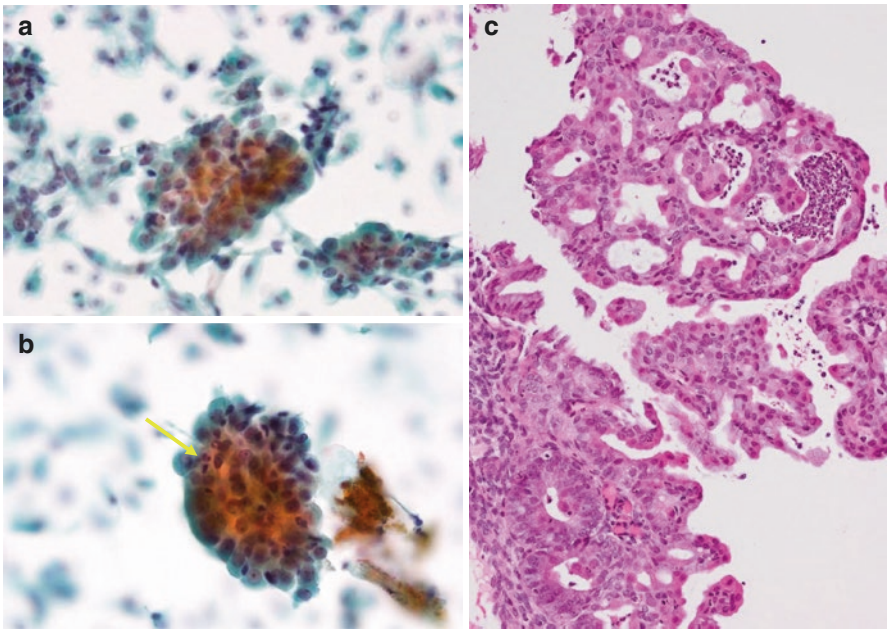

Fig. 11.9 EEC, G1, with microglandular pattern. Medium-sized epithelial cluster shows mild nuclear overlapping (**a**) and tiny irregular lumen (arrow) is seen in cluster (**b**). Corresponding to histologic preparation (**c**) show microglandular pattern and contain a number of neutrophils in lumens. (**a** and **b**: Papanicolaou stain, original magnification 40×, **c**: HE stain, original magnification 20×)

The method of evaluation of neoplastic epithelial clusters is mentioned in Chap. 5, as an algorithmic interpretational approach of endometrial cytology for the Yokohama System.

11.1.4 Explanatory Note

Several previous studies have identified genetic alterations of ECs, such as microsatellite instability and mutation in the *PTEN*, *PIK3CA*, *CTNNB1*, *ARID1A*, *KRAS*, *TP53* genes. In the Bokhman classification, each subtype shows characteristic frequencies of molecular alterations, with type I tumors having more mutation in genes for *PTEN*, *PIK3CA*, *CTNNB1*, *ARID1A*, *KRAS*, whereas type II having more *TP53* mutations [4].

Profiling the notable pattern of somatic genomic alterations, based on TCGA study revealed that EECs were divided into four molecular subtypes: ultramutated (POLE hotspot mutation), hypermutated (microsatellite instability), copy number low, and high copy number [7]. These four subtypes show characteristic gene mutations, histological features, clinical features, and prognosis [4, 5, 11, 12].

As mentioned in the definition, EECs are divided into three grades using the FIGO grading criteria in the fifth WHO Classification. When severe cellular atypia, inappropriate for architectural grade, is seen in more than 50% of tumor cells, G1 and G2 tumors are considered one grade higher. The cellular atypia of EEC is generally evaluated according to the degree of nuclear size, shape, anisonucleosis, pseudostratification and loss of polarity of nucleus, chromatin distribution, and nucleolus size and numbers. Zaino et al. defined large, pleomorphic nuclei with coarse chromatin, and large irregular nucleoli, as the notable atypia to raise a grade of tumors [13] (Fig. 11.10). Recently Norimatsu et al. evaluated nuclear morphometry by using an image analysis software, and observed that endometrial LBC samples exhibit an increase in nuclear enlargement, anisonucleosis, chromatin distribution and structure, nuclear shape, nuclear arrangement, and nucleolar size in comparison with EEC, G1, EEC, G3 and serous carcinoma [14]. Although the evaluation of cellular atypia is somewhat subjective, the objective measurement of nucleolar size could be indicative of cellular atypia and distinction between low-grade EEC and high-grade EEC in endometrial LBC samples [14].

In the fifth WHO Classification, EECs are divided into four molecular classifications: *POLE*-ultramutated EEC, mismatch repair (*MMR*)-deficient EEC, *p53*-mutant EEC, and no specific molecular profile (NSMP) EEC.

Among these four subgroups, *POLE*-ultramutated EEC, *MMR*-deficient EEC, and *p53*-mutant EEC exhibit high-grade histological appearance, and NSMP EC are

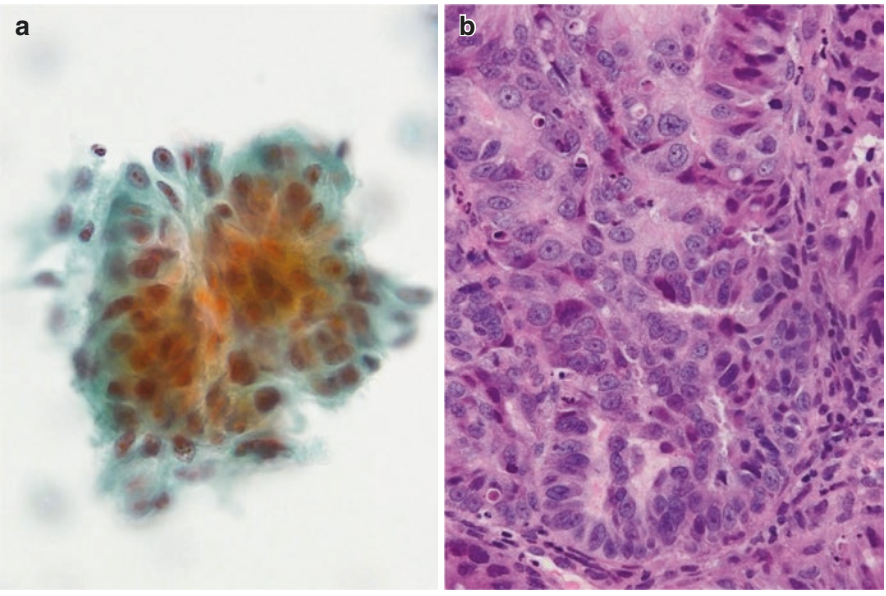

Fig. 11.10 EEC, G2, with severe nuclear atypia. Many tumor cells have enlarged nuclei with large and eosinophilic Nucleoli (**a**). Corresponding to histologic preparation shows an inconspicuous glandular pattern. (**b**) (**a**: Papanicolaou stain, original magnification 60×, **b**: HE stain, original magnification 40×)

mostly as low-grade feature with squamous differentiation or morules. However, the frequency of NSMP EC is approximately 30–40%, and other low-grade EECs belong to three different subgroups (Figs. 11.11, 11.12, 11.13 and 11.14). In contrast, high-grade EECs were found in all four subgroups. Although the morphological features of high-grade EECs are overlapped between these subgroups, clinical outcomes show distinctive differences [15]. However, *POLE*-ultramutated EEC has an excellent prognosis. This subtype shows frequently increasing nuclear size, irregular nuclear contours, striking hyperchromasia, prominent nucleoli [16, 17]. As mentioned above, accurate evaluation of the degree of nuclear atypia is considered an indicative finding in estimating the biological features of tumors [13, 18], but in the diagnosis of EEC, an approach from the aspect of tumor morphology alone may be insufficient [19, 20]. The algorithm for diagnosis of EEC, using molecular and immunohistochemical surrogate markers for each subgroup such as *POLE* hotspot mutation, *MSI* assay, *MMR*-deficient, *TP53* mutation, and *p53* immunohistochemistry, has also been proposed [21] (Figs. 11.15, 11.16, 11.17, 11.18, 11.19 and 11.20).

Recently in LBC endometrial sample, *PTEN* mutation and loss of expression, *p53* overexpression and β-catenin nuclear expression could be evaluated by immunocytochemistry or molecular techniques [22–24]. Application of DNA analysis using LBC endometrial samples has been reported [25], and it will be possible to consider cytological approaches including immunocytochemical and molecular analysis in near future.

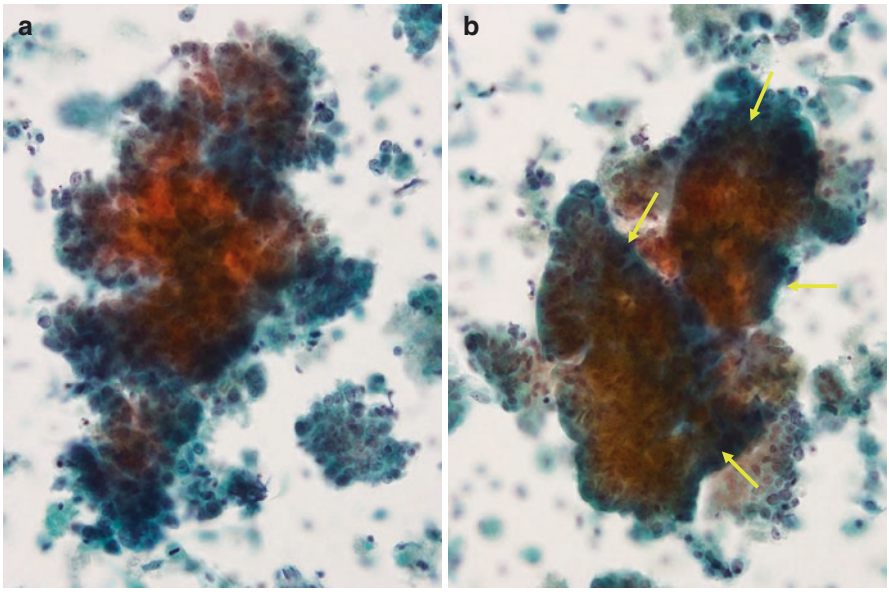

Fig. 11.11 EEC, G2. This cytological preparation was obtained from a 50 y-o woman. Clusters show irregular shapes and marked overlapping (**a** and **b**). Irregularly shaped lumens are seen within a cellular cluster (arrows). (**b**) (Papanicolaou stain, original magnification **a** and **b**: 40×)

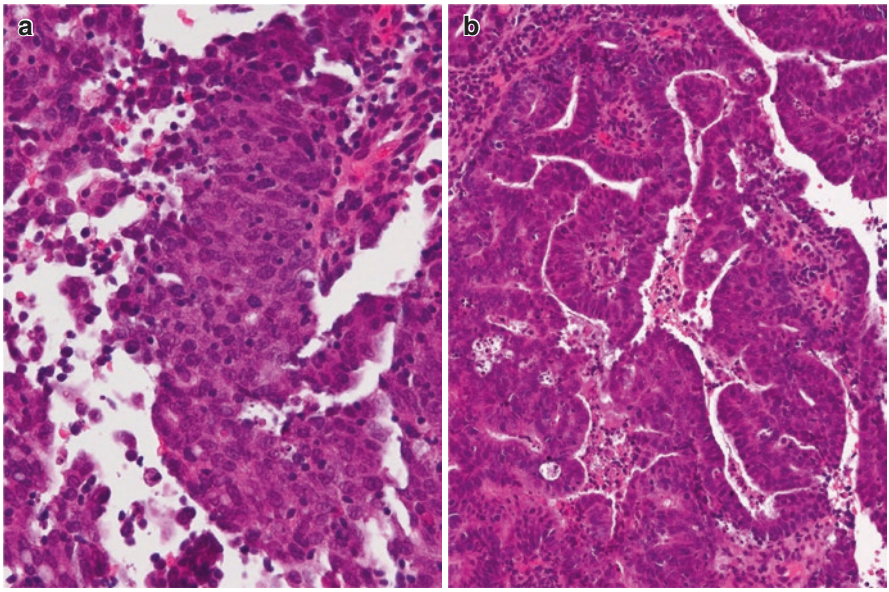

Fig. 11.12 EEC, G2. Histological specimen corresponding to Fig. 11.11. Solid nest with lymphocytes infiltration is present (**a**). Complex papillary and glandular architecture can be seen (**b**). (HE stain, original magnification **a**: 40×, **b**: 20×)

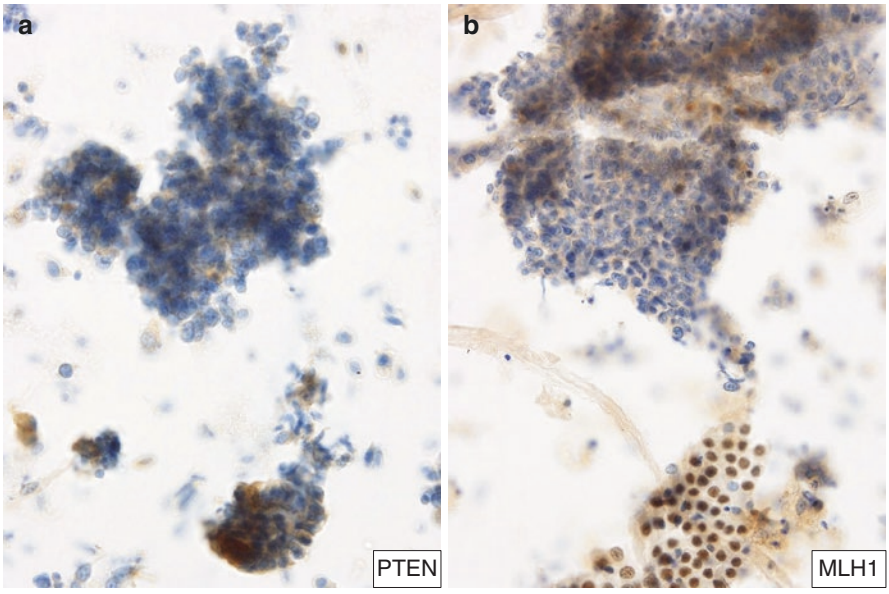

Fig. 11.13 EEC, G2. Same sample as Fig. 11.12. (**a**): On immunocytochemistry (ICC), clusters with loss of PTEN expression (upper), with a small number of PTEN expressing stromal cells can be seen (lower). (**b**): tumor cells show complete loss of MLH-1 expression (upper). MLH-1 expressing atrophic endometrial epithelial cells can be seen (lower). (ICC, original magnification **a** and **b**: 40×)

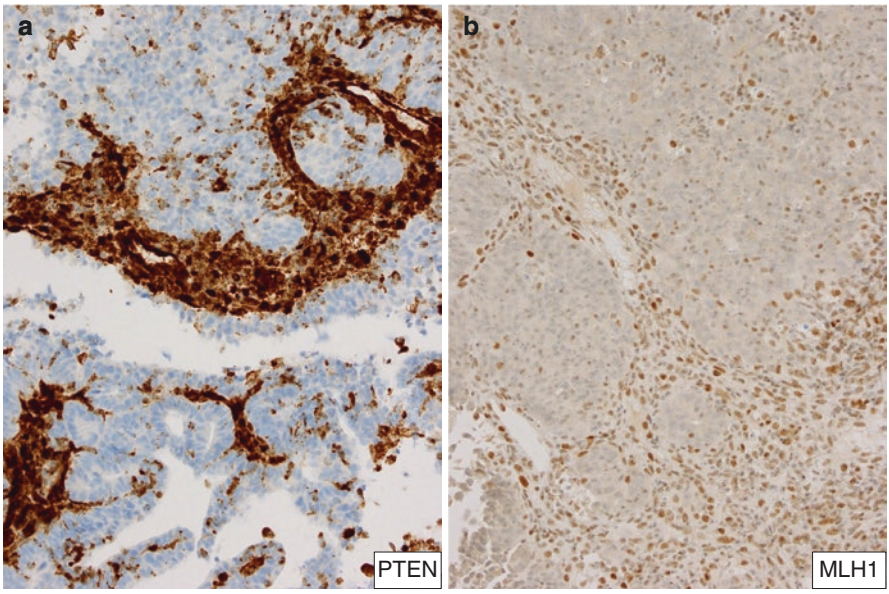

Fig. 11.14 EEC, G2. Same sample as Fig. 11.11. On immunohistochemistry (IHC), neoplastic glands show complete PTEN loss of expression (**a**) and loss of MLH-1 expression (**b**) (IHC, original magnification **a** and **b**: 20×)

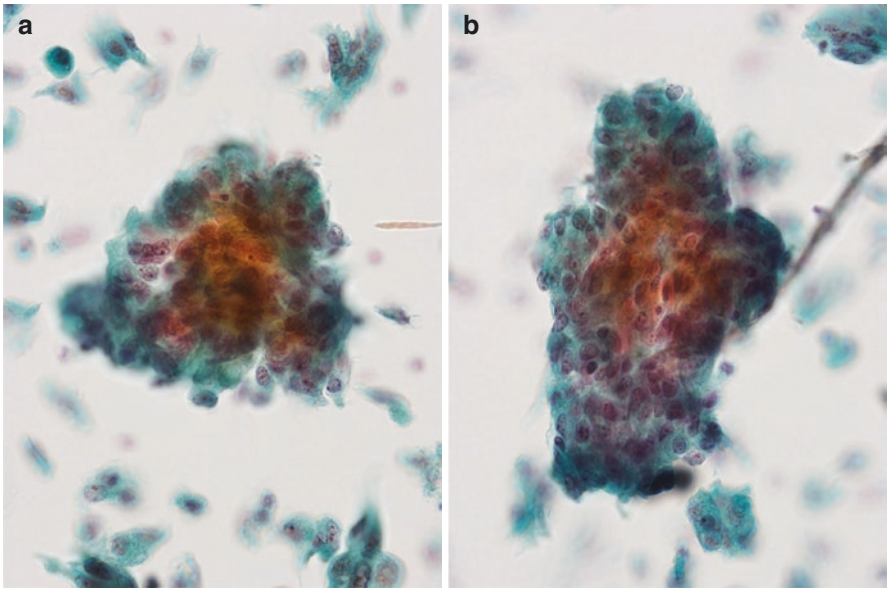

Fig. 11.15 EEC, G3. Nuclear overlapping and loose connection in cluster can be seen (**a**). Nuclei show enlarged, various shapes, and display fine granular chromatin and conspicuous nucleoli (**b**). (Papanicolaou stain, original magnification **a** and **b**: 60×)

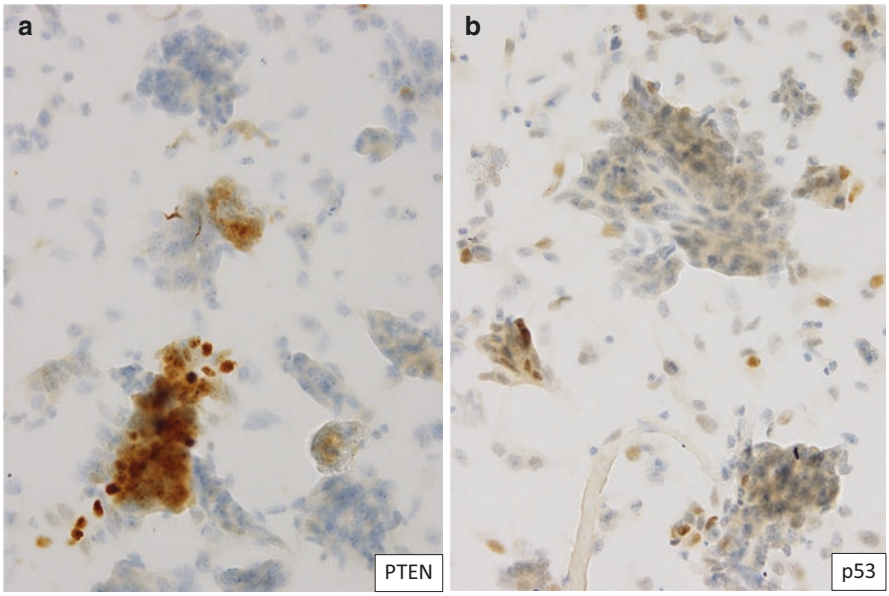

Fig. 11.16 EEC, G3 (same sample as Fig. 11.15) (**a**): On ICC, neoplastic clusters with loss of PTEN expression, with numbers of PTEN expressing stromal cells, can be seen (bottom) (**b**): almost neoplastic cells exhibit weak expression of *p*53. (ICC, original magnification **a** and **b**: 40×)

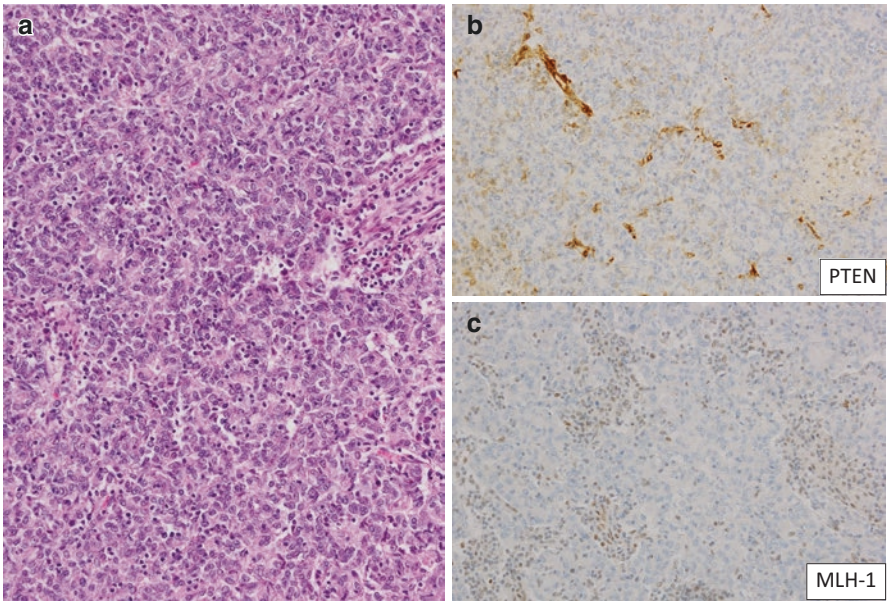

Fig. 11.17 EEC, G3 (same sample as Fig. 11.15). Corresponding to histologic preparation (**a**) shows solid nests with lymphocytes infiltration. (**b**): Tumor nests show PTEN loss of expression. (**c**): Tumor nests show with complete loss of MLH-1 expression. (**a**: HE stain, original magnification 20×, **b** and **c**: IHC, original magnification 20×)

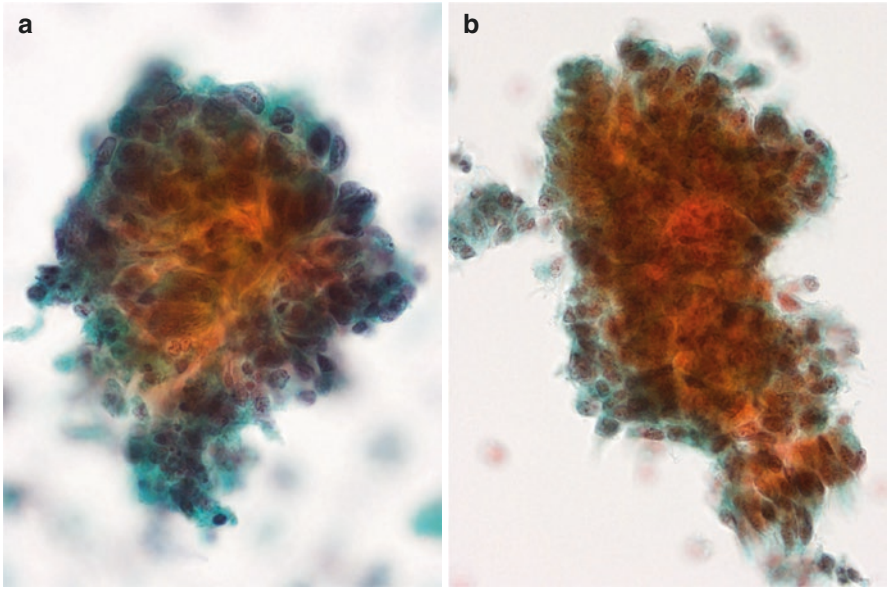

Fig. 11.18 EEC, G3. Cluster shows an irregular shape. Significant nuclear overlapping in cluster can be seen. Nuclei show enlarged, various shapes, and display granular chromatin and conspicuous nucleoli. (Papanicolaou stain, original magnification **a** and **b**: 60×)

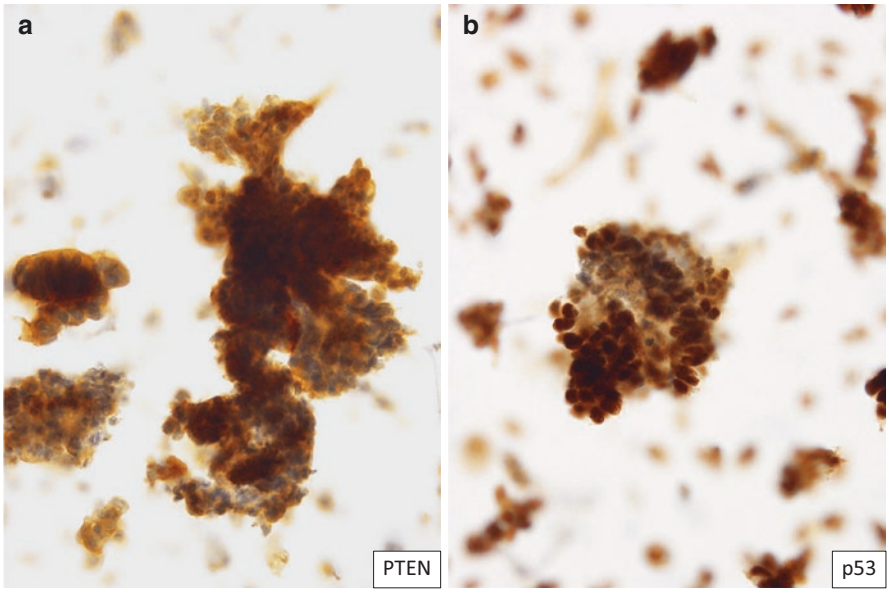

Fig. 11.19 EEC, G3 (same sample as Fig. 11.18). (**a**): On ICC, PTEN expressing clusters. (**b**): almost all tumor cells exhibit strong and diffuse nuclear expression of *p*53. (ICC, original magnification **a** and **b**: 40×)

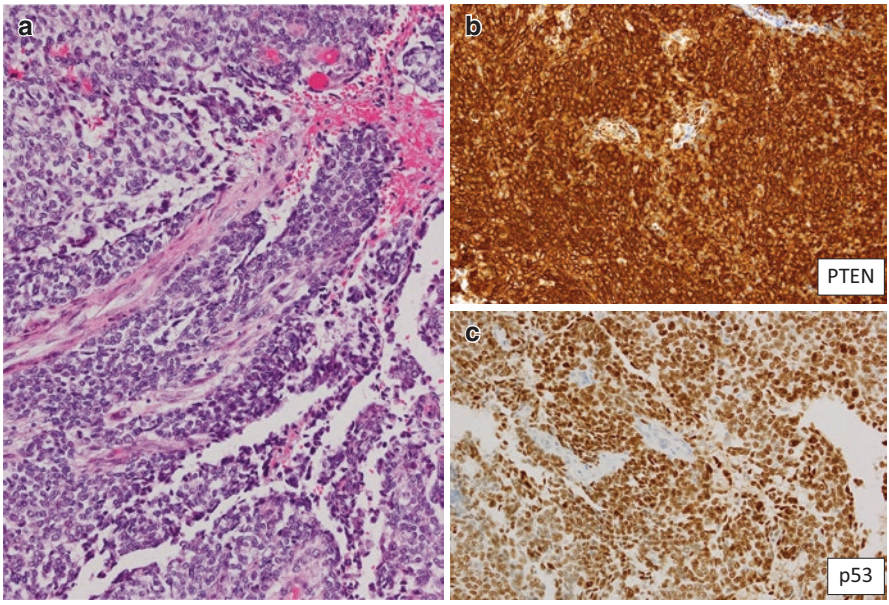

Fig. 11.20 EEC, G3 (same sample as Fig. 11.18). Corresponding histological specimen (**a**) shows sheet-like solid nests. (**b**): Tumor nests show PTEN expression. (**c**): Tumor nests show exhibit strong and diffuse nuclear expression of *p*53. (**a**: HE stain, original magnification 20×, **b** and **c**: IHC, original magnification 20×)

11.2 Serous Carcinoma, Including Serous Endometrial Intraepithelial Carcinoma (SEIC)

11.2.1 Background

In the 1980s, ECs were classified as estrogen-dependent Type I or estrogen-independent Type II. G1 and G2 EECs, which develop from endometrial atypical hyperplasia/endometrioid intraepithelial neoplasia (EIN), are representative subtypes of Type I. On the other hand, serous carcinoma (SC) and EEC, G3, are typical subtypes of Type II. However, Type II tumors are infrequent and often develop in postmenopausal women with underlying atrophic endometrium [26].

SC was first described by Hendrickson et al. in 1982, and has aggressive biological features and poor prognosis [27, 28]. It has a relatively low prevalence, accounting for 2–10% of all ECs, and approximately half of all EC-related deaths [29]. Some studies have reported that *p*53 mutations are common in endometrial serous carcinoma, and occur early in carcinogenesis [30, 31]. Recently, the Cancer Genome Atlas (TCGA) study placed SC in the copy-number-high subgroup [32].

11.2.2 Definition

In the fifth edition of the WHO classification in 2020, SC is defined as a carcinoma with diffuse, marked nuclear pleomorphism, and a typical papillary and/or glandular growth pattern. In addition to arising in the atrophic endometrium, development within endometrial polyps is also possible [33].

SC shows papillary structures with delicate fibrovascular stroma or thick fibrous strands and, sometimes, tubular structures or slit-like spaces. Tubular structures composed of columnar tumor cells needing to be differentiated from ECC are sometimes recognized. A solid pattern can also be present. Tumor cells are polygonal to columnar and show high-grade nuclear atypia, with a high N/C ratio. Psammoma bodies are occasionally encountered [34].

11.2.3 Cytologic Diagnostic Criteria (Figs. 11.21, 11.22, 11.23, 11.24, 11.25, 11.26 and 11.27)

- Frequent hemorrhagic background.
- Frequent occurrence of small to medium-sized 3D clusters showing irregular structure.
- Nuclear overlapping of three or more layers and irregular cellular arrangement in the clusters.
- Light-green cytoplasm in almost all tumor cells.
- Nuclei show the increased size and marked pleomorphism with coarse nuclear chromatin and large and eosinophilic nucleoli; cells with bizarre nuclei and/or multinucleated syncytial tumor cells are frequently found.
- Mitotic activity is usually high and atypical mitoses are easily recognized.
- Psammoma bodies are present in approximately 30% of cases.

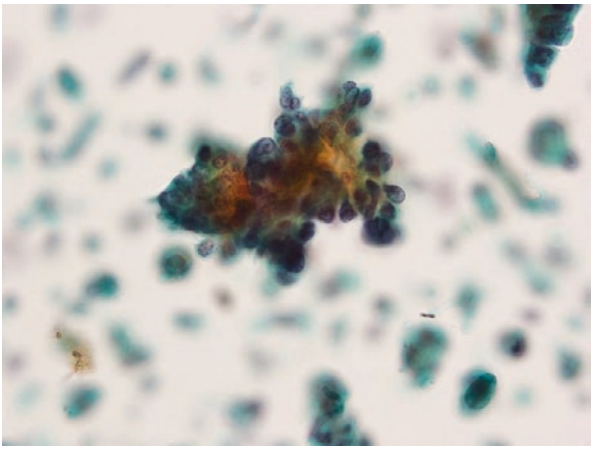

Fig. 11.21 SC. Irregularly shaped 3D cluster of tumor cells showing disordered cellular arrangement. (Papanicolaou stain, original magnification 40×)

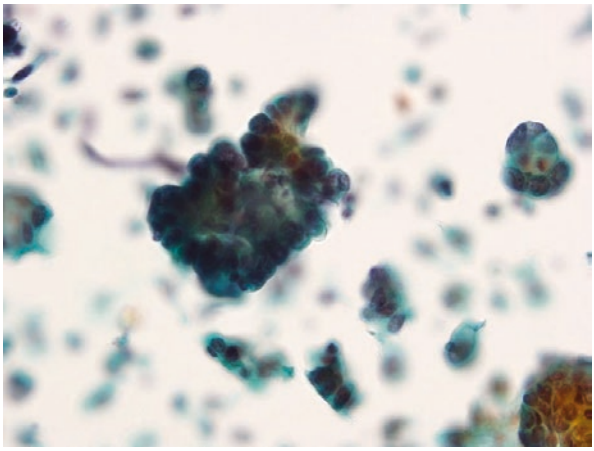

Fig. 11.22 Serous carcinoma. Tumor cell clusters are small to medium-sized and show nuclear overlapping of three or more layers. (Papanicolaou stain, original magnification 40×)

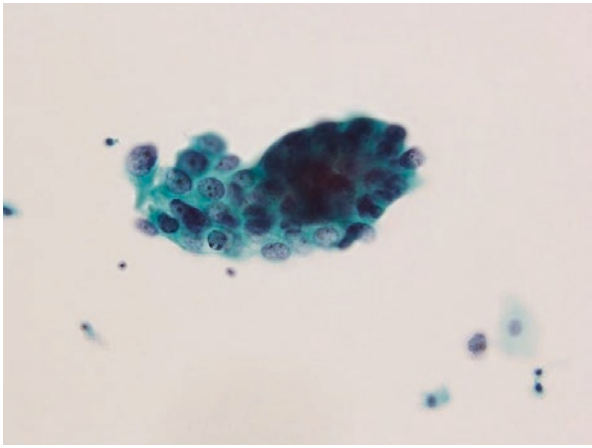

Fig. 11.23 SC. Tumor cells with light-green cytoplasm show increased N/C ratio, Hyperchromasia, conspicuous nucleoli, and pleomorphism. (Papanicolaou stain, original magnification 40×)

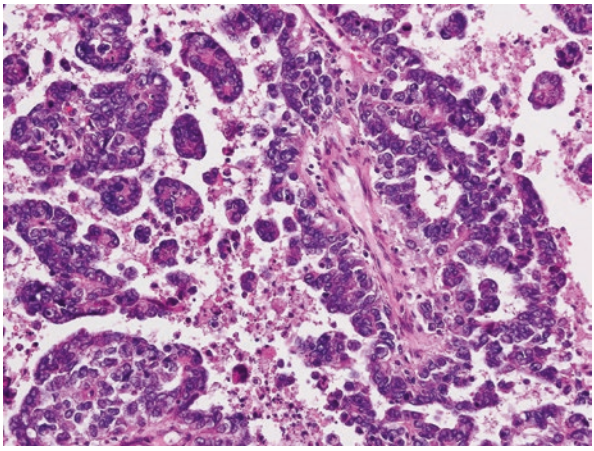

Fig. 11.24 SC. Corresponding histologic preparation shows a complex papillary pattern. Dissociated tumor cells and necrotic debris are also seen. (HE stain, original magnification 20×)

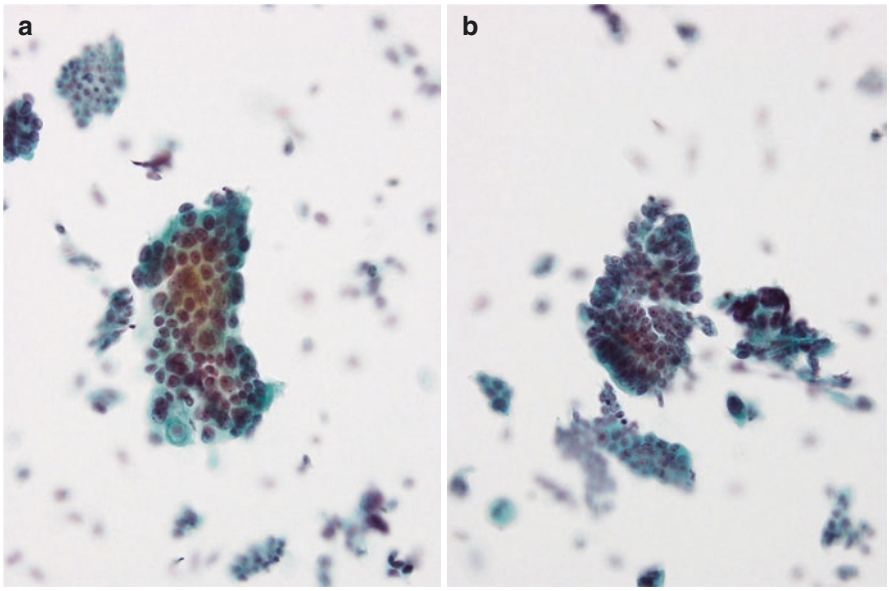

Fig. 11.25 SC (tiny lesion). 60 y-o patient (**a**): a medium-sized irregular cluster of tumor cells from small lesion of serous carcinoma shows pleomorphic, enlarged nuclei. (**b**): small-sized clusters show nuclear overlapping of more than three layers. (Papanicolaou stain, original magnification **a** and **b**: 40×)

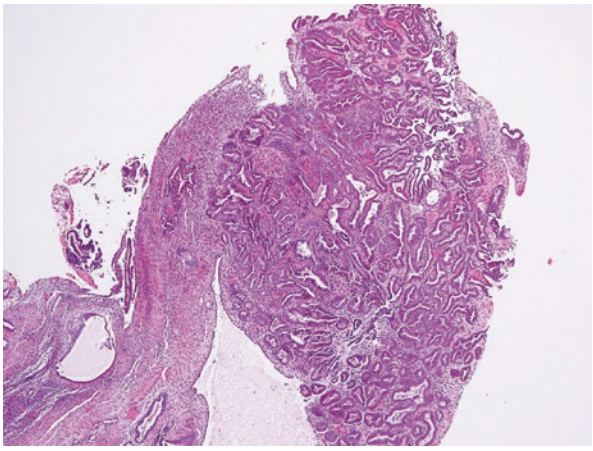

Fig. 11.26 SC (tiny lesion). Corresponding histologic preparation shows complex papillary and tubular structures. Tumor is confined to an endometrial polyp and 4 mm in maximum size. (HE stain, original magnification 4×)

In the fourth edition of the WHO classification, serous endometrial intraepithelial carcinoma (SEIC) is described as an immediate precursor lesion of SC that has no stromal invasion [35]. Similar to SC, the background consists of atrophic endometrium and endometrial polyps. SEIC and serous carcinoma less than 1 cm in maximum size, without myometrial and vascular invasion or extrauterine metastases, have a favorable prognosis [36–38]. Unlike EEC, there is a potential for

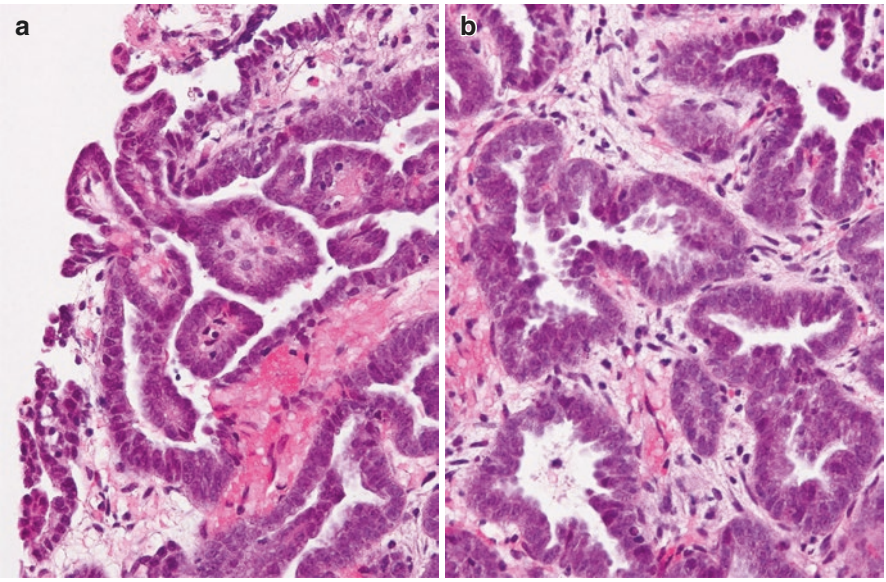

Fig. 11.27 SC (tiny lesion). Same case as Fig. 11.26. (**a**): showing small papillary structures with fibrovascular stroma. (**b**) tumor cells show enlarged and pleomorphic nuclei. (HE stain, original magnification **a** and **b**: 20×)

extrauterine metastasis to the abdominal cavity. In the fifth edition of the WHO classification in 2020, SEIC is included in the SC group. SEIC is synonymous with SC; and should therefore be used as a descriptive, not diagnostic term [39]. Endometrial cytology plays an important role in diagnosing SEIC, which is often asymptomatic and has a small size.

In SEIC, tumor cells replace the normal endometrial lining (refer to Chap. 12). In addition to showing a tubular structure that retains the original glandular shape, small papillary and sieve-like structures are also seen. There may be a distinctive front at the non-neoplastic endometrial glandular epithelium. Tumor cells are polygonal, hobnail-like, and columnar. Nuclear atypia is marked, similar to that of SC, and the N/C ratio is high. Neoplastic nuclei are 4–5 times larger than atrophic endometrial glandular nuclei in the background.

The cytologic findings in SEIC are almost the same as those of SC described above, except that the background is clear and the degree of nuclear overlapping is often one or two layers [40, 41] (Figs. 11.28, 11.29, 11.30 and 11.31).

11.2.4 Explanatory Note

Zheng et al. reported that approximately 90% of SCs show mutation-pattern overexpression of *p*53 protein, with a frequency of *TP53* gene mutations of 96%. The estrogen receptor (ER) is expressed in less than 30% of cases, and insulin-like

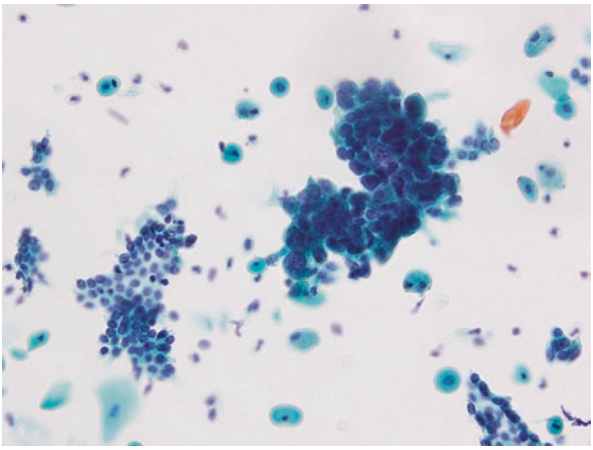

Fig. 11.28 SEIC. Medium-sized clusters derived from SEIC, show nuclear overlapping of more than three layers, in contrast to an atrophic endometrial cell cluster (lower left). (Papanicolaou stain, original magnification 40×)

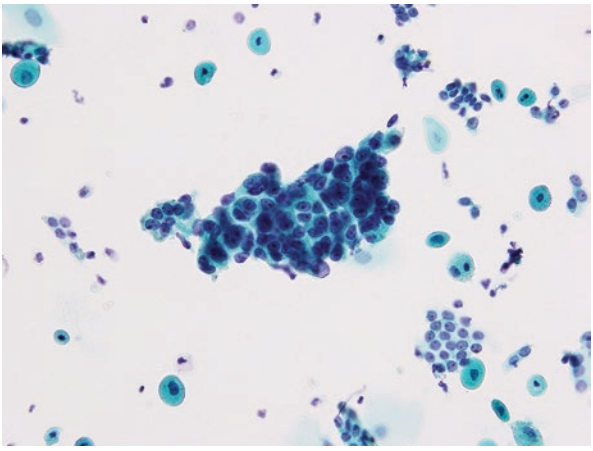

Fig. 11.29 SEIC. Medium-sized irregular cluster of tumor cells from SEIC shows enlarged and pleomorphic nuclei. (Papanicolaou stain, original magnification 40×)

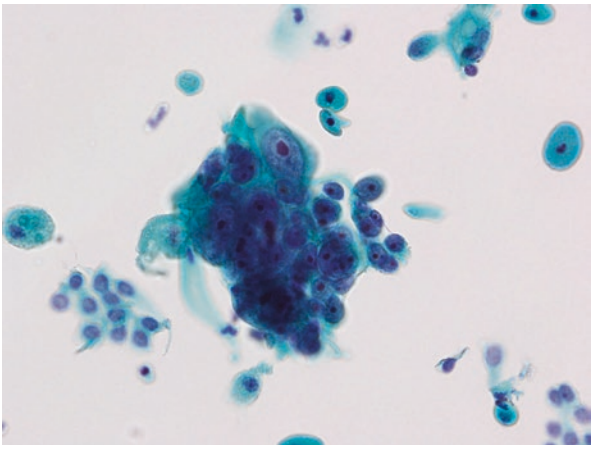

Fig. 11.30 SEIC. Large and eosinophilic nucleoli are seen in many tumor cells of SEIC. (Papanicolaou stain, original magnification 60×)

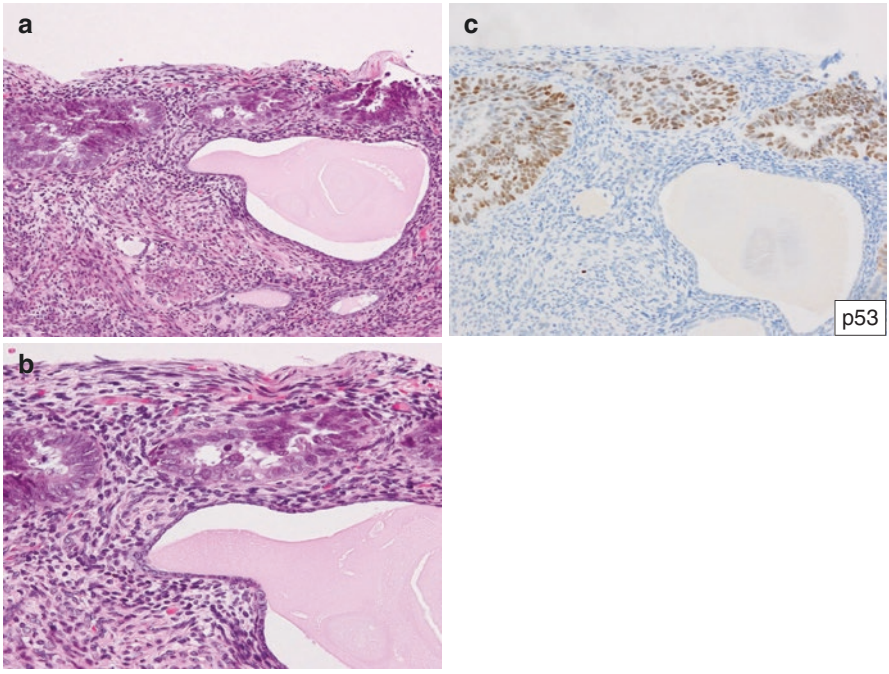

Fig. 11.31 SEIC. (**a**): corresponding histologic preparation Figs. 11.10, 11.11 and 11.12, shows glandular structures with no evidence of stromal invasion. (**b**): tumor cells are confined to the glands in atrophic endometrium and detached tumor cell clusters. (**c**): almost all tumor cells exhibit strong and diffuse nuclear expression of *p*53. (**a** and **b**: HE stain, original magnification 20×, **c**: IHC, original magnification 20×)

growth factor II mRNA-binding protein 3 (IMP3), which is an oncofetal protein expressed during the fetal period, is overexpressed in 91% of cases. Furthermore, the labeling index of Ki-67 is as high as 30–50% or more, and p16 expression is observed in more than 90% of cases [39, 42, 43].

When diagnosing SC, marked nuclear atypia and irregular-shaped tumor cell clusters are important clues. However, villoglandular-type EEC, high-grade EEC, and clear cell carcinoma should be differentiated from SC.

Using LBC preparations, it is easy to prepare unstained samples for ancillary tests, such as immunocytochemistry. Positive stains for *p*53, p16, ER, and IMP3, can be used to support the diagnosis (Figs. 11.32 and 11.33).

SEIC also frequently shows mutation-pattern overexpression of *p*53 protein, and *TP53* gene mutations are seen in 63–72% of cases. ER are also expressed in less than 30% of cases, similar to serous carcinoma.

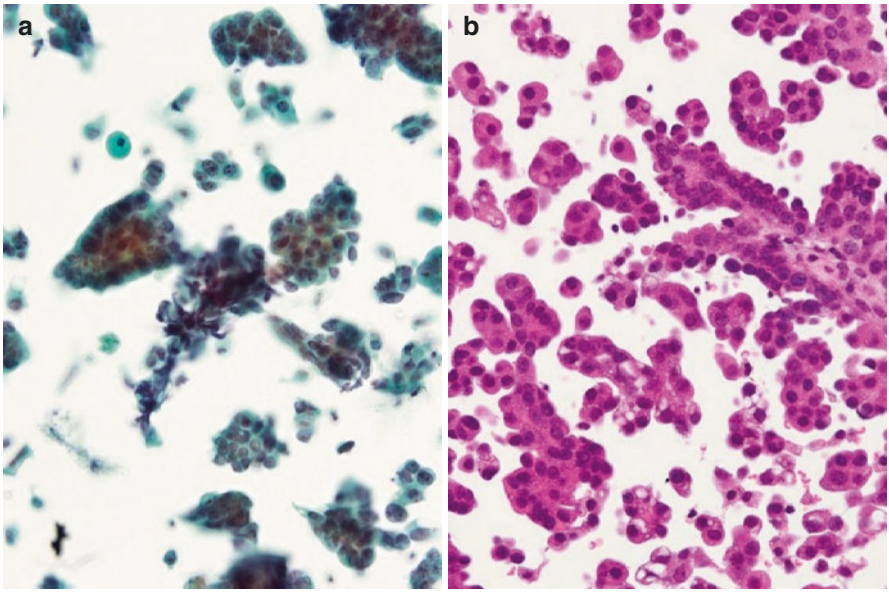

Fig. 11.32 SC. (**a**): small to medium-sized irregular clusters of tumor cells show enlarged, pleomorphic nuclei, with conspicuous nucleoli, and overlapping of more than three layers. (**b**): corresponding histologic preparation shows papillary structures and detached tumor cells clusters. (**a**: Papanicolaou stain, original magnification 40×, **b**: HE stain, original magnification 20×)

Endometrial glandular dysplasia (EmGD), a precancerous lesion of endometrial serous cancer, has been proposed to be a possible precursor of serous cancer (both SEIC and SC) [39, 44], judging from the occurrence of *p*53 abnormalities in the resting atrophic endometrium (so-called "*p*53 signature") [45]. This condition shows coexistence and transition from the surrounding atrophic endometrial glands or SEIC. The histopathologic features of EmGD consist of nuclear hyperchromasia with inconspicuous nucleoli and no atypical mitoses. The size of the lesion may be as small as 1 mm or less. Many of them show a mutation-pattern overexpression of *p*53 protein, and the frequency of *TP53* gene mutations is 43%. ER and PgR are expressed in 70–95%, 60–90% of cases, respectively. Cytological examination plays an important role in the detection of this state and may assist appropriate clinical management in order to prevent the development of endometrial serous cancer (Figs. 11.34, 11.35 and 11.36).

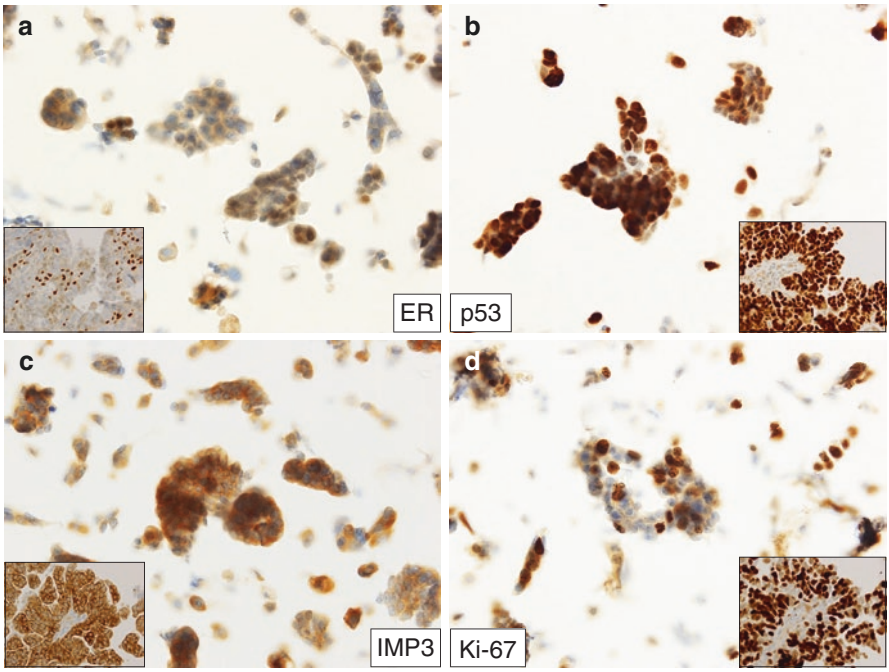

Fig. 11.33 SC (same cases as Fig. 11.32). Immunocytochemical staining (**a**): tumor cells do not express or show reduced expression of ER (inset; IHC staining) (**b**): almost all tumor cells exhibit strong and diffuse nuclear expression of *p*53 (inset; IHC staining) (**c**): almost all tumor cells show cytoplasmic expression of IMP3 (inset; IHC staining). (**d**): increased ratio of Ki-67 labeled tumor cells in cluster (inset; IHC staining, original magnification 20×) (ICC, original magnification **a**–**d**: 40×)

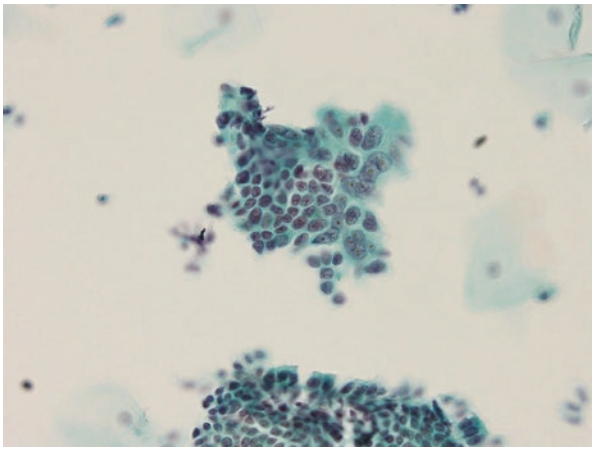

Fig. 11.34 A sheet-like epithelial cell cluster is seen. Epithelial cells show increased nuclear size with anisonucleosis and hyperchromasia, suggesting neoplastic nature. (Papanicolaou stain, original magnification 40×)

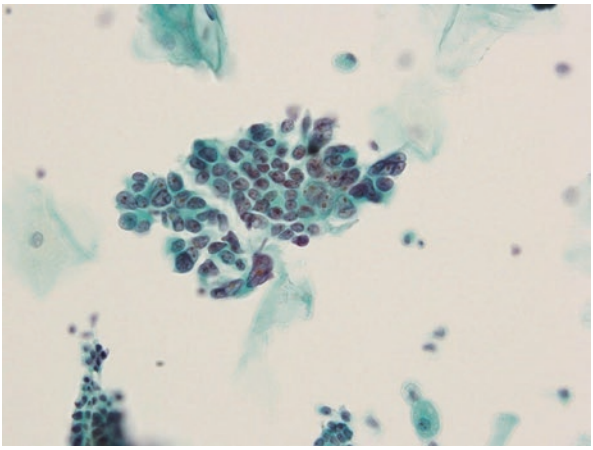

Fig. 11.35 Same cases as Fig. 11.14; showing mild nuclear overlapping. (Papanicolaou stain, original magnification 40×)

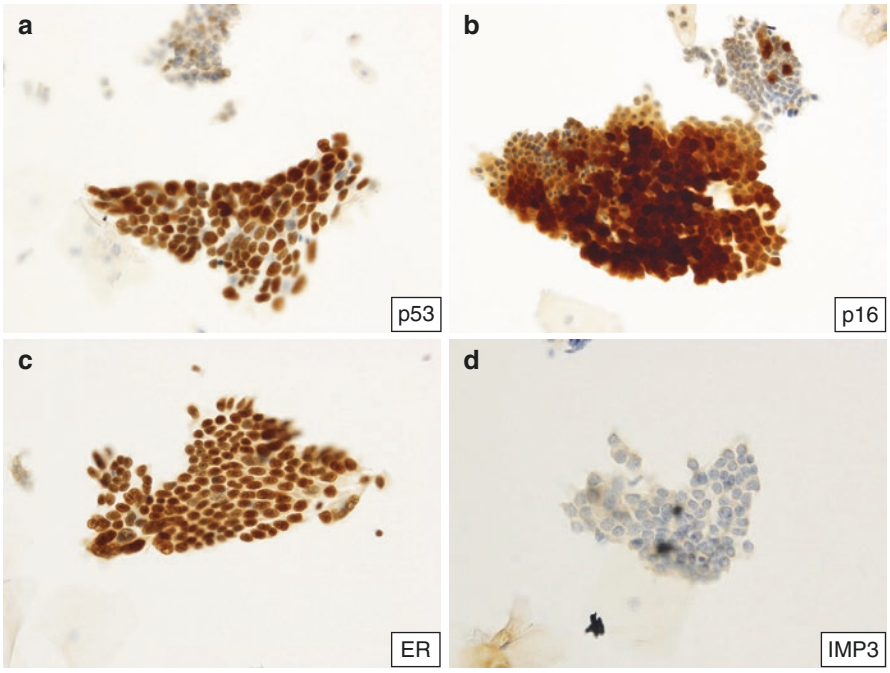

Fig. 11.36 Cytologic preparation from the same sample of Figs. 11.34 and 11.35, (**a**): ER is expressed in almost all cells. (**b**): almost all tumor cells exhibit strong and diffuse expression of p16. (**c**): almost all tumor cells exhibit strong and diffuse nuclear expression of *p*53. (**d**): IMP3 is not expressed. (ICC, original magnification **a**–**d**: 40×)

11.3 Clear Cell Carcinoma

11.3.1 Background

Clear cell carcinoma (CCC) was first described in 1973 and classified as an estrogen-independent endometrial carcinoma [46]. The prevalence of CCC is approximately 1–6%. Similar to SC, CCC occurs in patients aged 65 years or older, and postmenopausal irregular uterine bleeding is a frequent symptom. CCC tends to show a high nuclear grade and is associated with deep myometrial invasion and vascular invasion. Occasionally endometrial polyps occur. It is worth mentioning that the risk of venous thromboembolism increases in patients with CCC. Studies have reported the overall 5-year survival rate to range from 55% to 78% [47–49].

DeLair et al. reported that genetic mutations occur in *POLE*, *MMR-D*, and *p53* in endometrial CCC [50]. Although it had been considered a Type 2 endometrial carcinoma, its genomic profile shows that endometrial CCC can be regarded as a tumor with intermediate features between EEC and SC.

11.3.2 Definition

In the fifth edition of the WHO classification of 2020, CCC is defined as a carcinoma with a papillary, tubulocystic, and/or solid architectural pattern and variably pleomorphic, cuboidal, flat, or hobnail cells with clear or eosinophilic cytoplasm [49]. Nuclear atypia is generally moderate to severe, with anisonucleosis and distinct eosinophilic large nucleoli. Atypical mitoses are rarely seen. Deposits of basement membrane-like substances, including type IV collagen and laminin, are found in the stroma in form of eosinophilic hyalinized material [51, 52].

11.3.3 Cytologic Diagnostic Criteria (Figs. 11.37, 11.38, 11.39, 11.40 and 11.41)

- Sheet-like clusters or small papillary clusters with mild nuclear overlapping.
- Tumor cells have abundant and clear cytoplasm with oval to round nuclei with eosinophilic large nucleoli, and finely granular chromatin.
- Hobnail tumor cells protruding from the margin of clusters and a low N/C ratio.

11.3.4 Explanatory Note

EEC with clear cell areas secondary to secretory changes and squamous differentiation should be differentiated from CCC.

Immunohistochemically, endometrial CCC shows usually a negative or reduced expression of estrogen receptor (ER) and progesterone receptor (PgR), whereas it is frequently positive for hepatocyte nuclear factor-1 beta (HNF-1β) and Napsin A;

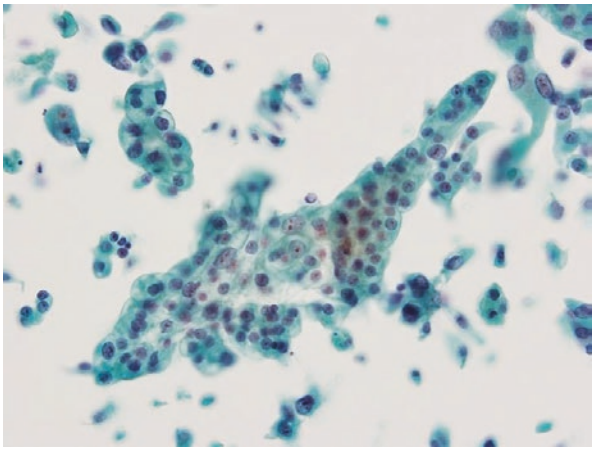

Fig. 11.37
CCC. Irregularly shaped sheet-like cluster of tumor cells is seen. Almost all tumor cells have abundant clear cytoplasm. (Papanicolaou stain, original magnification 40×)

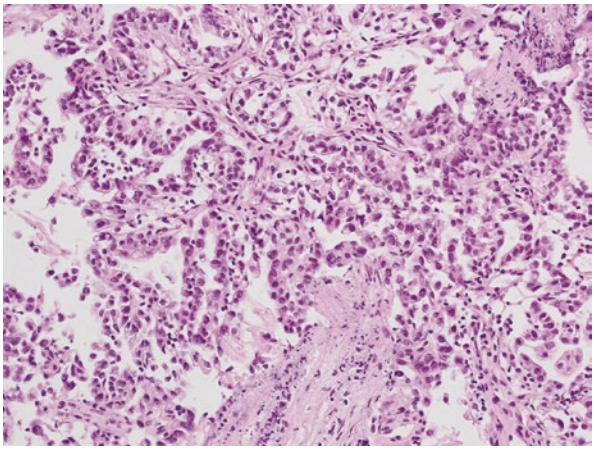

Fig. 11.38
CCC. Corresponding histologic preparation shows a complex papillary pattern and tubular structures. (HE stain, original magnification **a** and **b**: 20×)

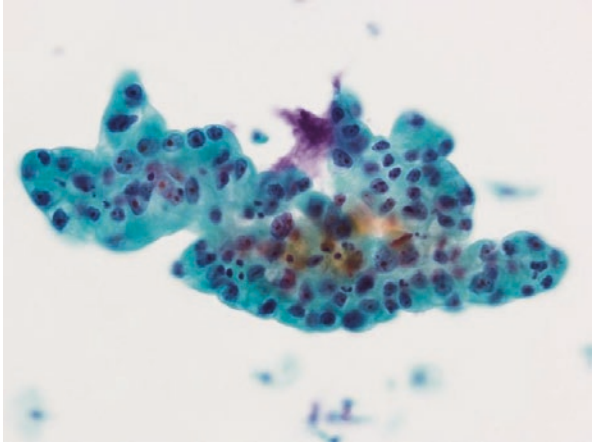

Fig. 11.39 CCC. Tumor cells have abundant clear or pale eosinophilic cytoplasm, and also show increased nuclear size with, anisonucleosis. (Papanicolaou stain, original magnification 40×)

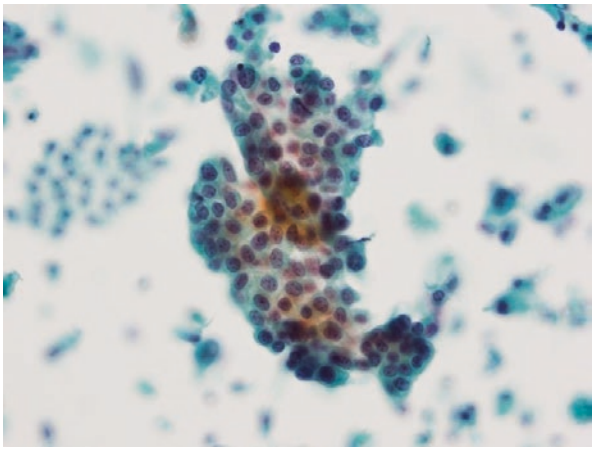

Fig. 11.40 CCC. Tumor cell cluster shows mild nuclear overlapping. (Papanicolaou stain, original magnification 40×)

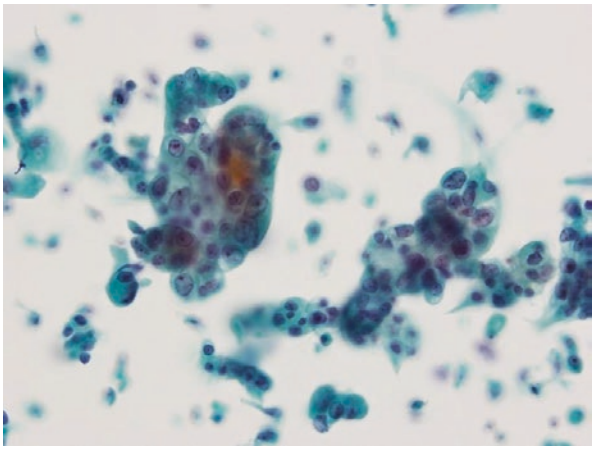

Fig. 11.41 CCC. Tumor cell clusters show mild nuclear overlapping. Tumor cells show. Increased nuclear size, pleomorphism, fine granular chromatin, and conspicuous nucleoli. (Papanicolaou stain, original magnification 40×)

these frequencies are 67–100% and 56–93%, respectively. Overexpression of *p*53 is found in approximately 22–72% of these cases [49, 53]. A study by Lim et al. reported that the positivity of HNF-1β, Napsin A, ER, and PgR was 43%, 14%, 86%, and 75%, respectively, in cases of EEC with clear cell areas [54]. Therefore, the use of immunocytochemical panels composed of HNF-1β, Napsin A, ER, and PgR is useful for distinguishing EEC with clear cell areas from CCC. However, it has also been reported that HNF-1β expression tends to be also frequent in SC and high-grade EEC, and it is hence necessary to pay attention to the differential diagnoses (Figs. 11.42 and 11.43).

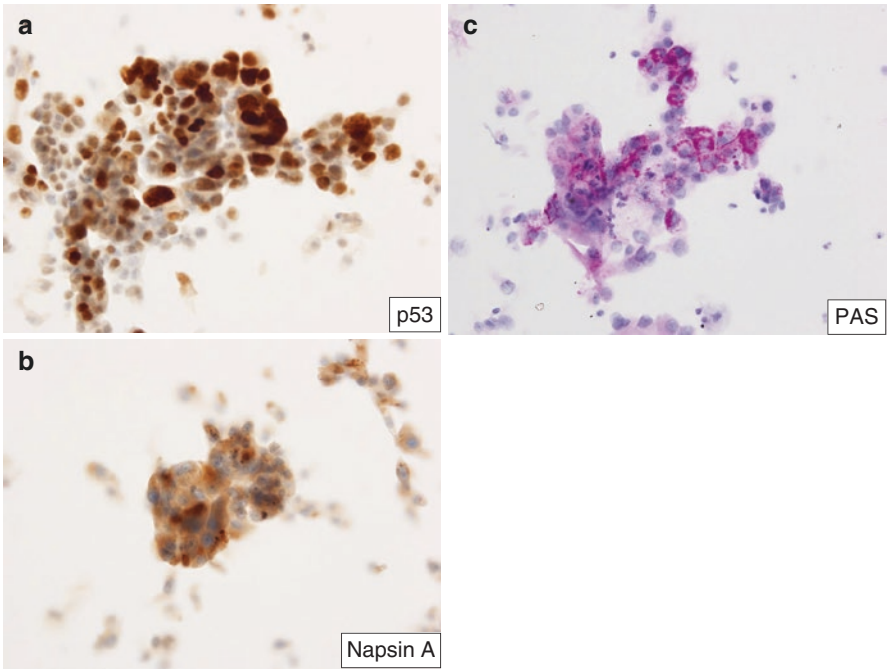

Fig. 11.42 CCC. Cytologic preparation from the same sample of Figs. 11.39, 11.40 and 11.41, (**a**): approximately half of tumor cells exhibit strong nuclear expression of *p*53. (**b**): tumor cells are stained for Napsin A. (**c**): tumor cells have PAS-positive glycogen in cytoplasm. (**a** and **b**: ICC, original magnification 40×, **c**: PAS reaction, original magnification 40×)

The Arias-Stella reaction (ASR) and metaplastic changes due to hormonal or irritative stimulation are also difficult to differentiate from CCC. Because these are benign lesions, overdiagnosis should be avoided. In ASR, epithelial cell clusters are composed of cells with clear or vacuolated abundant cytoplasm containing glycogen. The nuclei show some degree of atypia, with an irregular shape, anisonucleosis, relative hyperchromasia, and presence of intranuclear cytoplasmic inclusions [55]. Philip et al. reported that HNF-1β and Napsin A are highly expressed in ASR (100% and 96%, respectively). Expression of the ER and PgR is also reduced or absent [56]. Because of the overlapping IHC profile of ASR, immunohistochemical studies for differentiated CCC are limited. Clinical information, such as the presence or absence of pregnancy or hormonal drug use, is important. On the other hand, metaplastic changes with large nucleoli mimicking CCC are positive for ER, PgR, and negative for Napsin A and HNF-1β. This expression pattern is a useful ancillary finding for distinguishing CCC (Figs. 11.44 and 11.45).

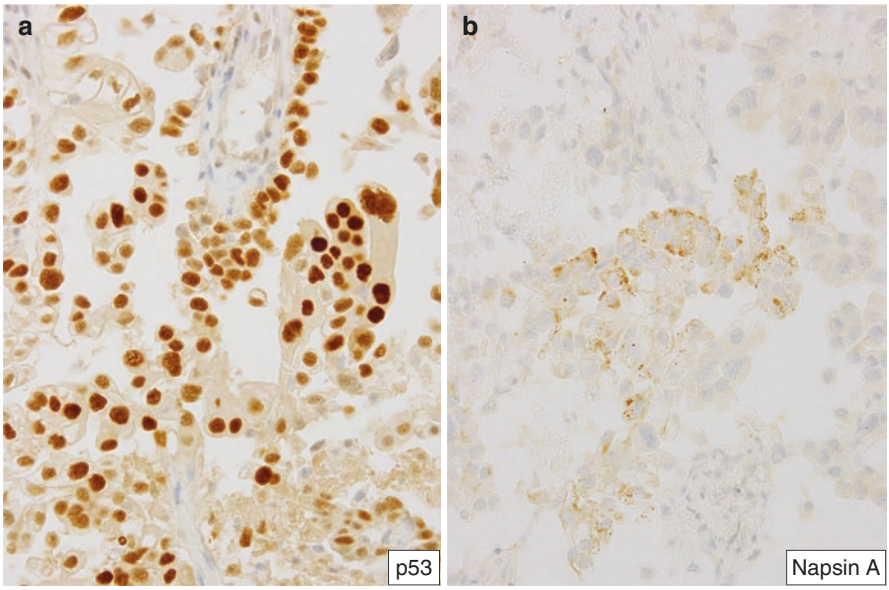

Fig. 11.43 CCC. Corresponding histologic preparation Figs. 11.39, 11.40 and 11.41, (**a**): approximately almost tumor cells exhibit strong nuclear expression of *p*53. (**b**): tumor cells are stained for Napsin A. (IHC, original magnification **a** and **b**: 20×)

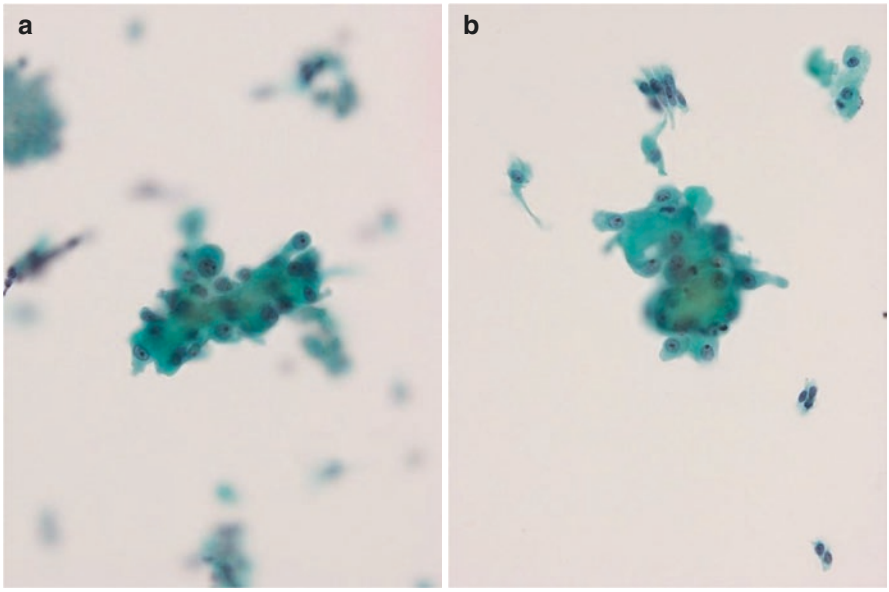

Fig. 11.44 (**a**) Metaplastic epithelial cells with abundant pale eosinophilic cytoplasm should be differentiated from CCC. (**b**) These epithelial cells show nuclear enlargement with prominent nucleoli. (Papanicolaou stain, original magnification **a** and **b**: 40×)

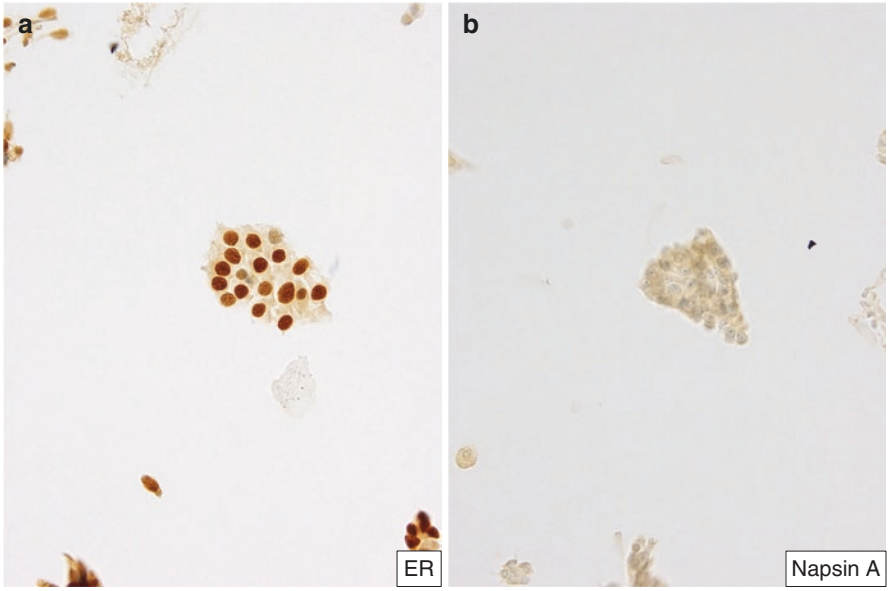

Fig. 11.45 Cytologic preparation from the same sample of Fig. 11.44, (**a**): approximately almost all epithelial cells show expression of ER. (**b**): Napsin A is not expressed. (ICC, original magnification **a** and **b**: 40×)

References

1. Bosse T, Lortet-Tieulent J, Davidson B, et al. Endometrioid carcinoma of the uterine corpus. In: WHO Classification of Tumor Editorial Board, editor. WHO classification of tumor of female reproductive organs. 5th ed. Lyon: IARC Press; 2020. p. 252–5.
2. Ellenson LH, Ronnett BM, Soslow RA, et al. Endometrial carcinoma. In: Kurman RJ, Ellenson LH, Ronnett BM, editors. Blaustein's pathology of the female genital tract. 7th ed. New York: Springer-Verlag; 2019. p. 473–533.
3. Bokhman JV. Two pathogenetic types of endometrial carcinoma. Gynecol Oncol. 1983;15:10–7.
4. Murali R, Soslow RA, Weigelt B. Classification of endometrial carcinoma: more than two types. Lancet Oncol. 2014;15:e268–78.
5. Kandoth C, Schultz N, Cherniack AD, et al. Integrated genomic characterisaion of endometrial carcinoma. Nature. 2013;497:57–73.
6. Norimatsu Y, Yanoh K, Kobayashi TK. The role of liquid-based preparation in the evaluation of endometrial cytology. Acta Cytol. 2013;57:423–35.
7. Yanoh K, Norimatsu Y, Munakata S, et al. Evaluation of endometrial cytology prepared with the Becton Dickinson SurePath™method:a pilot study by the Osaki study group. Acta Cytol. 2014;58:153–61.
8. Fulciniti F, Yanoh K, Karakitsos P, et al. The Yokohama system for reporting directly sampled endometrial cytology: the quest to develop a standardized terminology. Diagn Cytopathol. 2018;46:400–12.
9. Norimatsu Y, Kouda H, Kobayashi TK, et al. Utility of liquid-based cytology in endometrial pathology: diagnosis of endometrial carcinoma. Cytopathology. 2009;20:395–402.
10. Norimatsu Y, Yanoh K, Hirai Y, et al. A diagnostic approach to endometrial cytology by means of liquid-based preparations. Acta Cytol. 2020;64:195–207.

11. McAlpine J, Leon-Castillo A, Bosse T. The rise of novel classification system for endometrial carcinoma; integration of molecular subclasses. J Pathol. 2018;244:538–49.
12. Sugiyama Y, Gotoh O, Fukui N, et al. Two distinct tumorigenic processes in endometrial endometrioid adenocarcinoma. Am J Pathol. 2020;190:234–51.
13. Zaino RJ, Kurman RJ, Diana KL, et al. The utility of the revised International Federation of Gynecology and Obstetrics histological grading of endometrial adenocarcinoma using a defined nuclear grading system. Cancer. 1995;75:81–6.
14. Norimatsu Y, Irino S, Maeda Y, et al. Nuclear morphometry as an adjunct to cytopathologic examination of endometrial brushings on LBC samples: a prospective approach to combined evaluation in endometrial neoplasms and look alikes. Cytopathology. 2021;32:65–74.
15. Hoang LN, Kinloch MA, Leo JM, et al. Interobserver agreement in endometrial carcinoma histotype diagnosis varies depending on the Cancer genome atlas (TCGA)-based molecular subgroup. Am J Sure Pathol. 2017;41:245–52.
16. Hussein YR, Weigelt B, Levine DA, et al. Clinicopathological analysis of endometrial carcinomas harboring somatic *POLE* exonuclease domain mutations. Mod Pathol. 2015;28:505–14.
17. Conlon N, Da Cruz Paula ADC, Ashley CW, et al. Endometrial carcinomas with a "serous" component in young women are enriched for DNA mismatch repair deficiency, lynch syndrome, and *POLE* exonuclease domain mutations. Am J Surg Pathol. 2020;44:641–8.
18. Conlon N, Leitao MM Jr, Abu-Rustum NR, et al. Grading uterine endometrioid carcinoma. A proposal that binary is best. Am J Surg Pathol. 2014;38:1583–7.
19. Joehlin-Price A, Van Ziffle JV, Hills NK, et al. Molecularly classified uterine FIGO grade 3 endometrioid carcinomas show distinctive clinical outcomes but overlapping morphologic features. Am J Surg Pathol. 2021;45:421–9.
20. Bosse T, Nout RA, McAlpine JN, et al. Molecular classification of grade 3 endometrioid endometrial cancers identifies distinctive prognostic subgroups. Am J Surg Pathol. 2018;42:561–8.
21. Soslow RA, Tornos C, Park KJ, et al. Endometrial carcinoma diagnosis: use of FIGO grading and genomic subcategories in clinical practice: recommendations of the international society of gynecological pathologists. Int J Gynecol Pathol. 2019;38(Suppl 1):S64–S74.
22. Norimatsu Y, Miyamoto M, Kobayashi TK, et al. Diagnostic utility of phosphatase and tensin homolog, β-catenin, and p53 of endometrial carcinoma by thin-layer endometrial preparations. Cancer. 2008;114:155–64.
23. Di Lorito AD, Rosini S, Falo E, et al. Molecular alterations in endometrial archived liquid-based cytology. Diagn Cytopathol. 2013;41:492–6.
24. Di Lorito AD, Zappacosta R, Capanna S, et al. Expression of PTEN in endometrial liquid-based cytology. Acta Cytol. 2014;58:495–500.
25. Lu Li YW, Douville C, Cohen JD, et al. Evaluation of liquid from the Papanicolaou test and other liquid biopsies for detection of endometrial and ovaria cancers. Sci Transl Med. 2018;10:eaap8793. https://doi.org/10.1126/scitranslemd.aap8793.
26. Bokhman JV. Two pathogenetic types of endometrial carcinoma. Gynecol Oncol. 1983;15:10–7.
27. Hendrickson M, Ross J. Eifel, et al. Uterine papillary serous carcinoma. A highly malignant form of endometrial adenocarcinoma. Am J Surg Pathol. 1982;6:93–108.
28. Sherman ME, Rosenshein NB, Kurman RJ, et al. Uterine serous carcinoma. A morphologically diverse neoplasm with unifying clinicopathological features. Am J Surg Pathol. 1992;16:600–10.
29. Ueda SM, Kapp DS, Cheung MK, et al. Trends in demographic and clinical characteristics in women diagnosed with corpus cancer and their potential impact on the increasing number of deaths. Am J Obstet Gynecol. 2008;198:218.e1–6.
30. Moll UM, Chalas E, Auguste M, et al. Uterine papillary serous carcinoma evolves via a p53-driven pathway. Hum Pathol. 1996;27:1295–300.
31. Tashiro H, Isacson C, Levine R, et al. p53 gene mutation in uterine serous carcinoma and occurs early in their pathogenesis. Am J Pathol. 1997;150:177–85.

32. Kandoth C, Schultz N, Cherniack AD, et al. Integrated genomic characterizaion of endometrial carcinoma. Nature. 2013;497:57–73.
33. Ellenson LH, Parkash V, Stewart CJR. Serous carcinoma of the uterine corpus. In: WHO Classification of Tumor Editorial Board, editor. WHO classification of tumor of female reproductive organs. 5th ed. Lyon: IARC Press; 2020. p. 256–7.
34. Ellenson LH, Ronnett BM, Soslow RA, et al. Endometrial carcinoma. In: Kurman RJ, Ellenson LH, Ronnett BM, editors. Blaustein's pathology of the female genital tract. 7th ed. New York: Springer-Verlag; 2019. p. 473–533.
35. Zaino R, Carinelli SG, Ellenson LH, et al. Epithelial tumours and precursors. In: Kurman RJ, Carangiu ML, Herrington CS, et al., editors. WHO classification of tumor of female reproductive organs. 4th ed. Lyon: IARC Press; 2014. p. 125–35.
36. Carcangiu ML, Tan LK, Chambers JT. Stage IA uterine serous carcinoma: A study of 13 cases. Am J Surg Pathol. 1997;21:1507–14.
37. Wheeler DT, Bell KA, Kurman RJ, et al. Minimal uterine serous carcinoma. Diagnosis and clinicopathologic correlation. Am J Surg Pathol. 2000;24:797–806.
38. Hui P, Kelly M, O'Malley DM, et al. Minimal uterine serous carcinoma: a clinicopathologic study of 40 cases. Mod Pathol. 2005;18:75–82.
39. Zheng W, Xiang L, Fadare O, et al. A proposed model of endometrial serous carcinogenisis. Am J Surg Pathol. 2011;35:e1–e14.
40. Yasuda M, Katoh T, Hori S, et al. Endometrial intraepithelial carcinoma in association with polyp: review of eight cases. Diagn Pathol. 2013;8:25–31.
41. Umezawa T, Nomura K, Tsuchiya S, et al. Serous endometrial intraepithelial carcinoma. J Jpn Soc Clin Cytol. 2012;51:188–91. (in Japanese with English abstract).
42. Zheng W, Yi X, Fadare O, et al. The Oncofetal protein, IMP3. a novel biomarker for endometrial serous carcinoma. Am J Surg Pathol. 2008;32:304–15.
43. Yomelyanova A, Ji H, Shih IM, et al. Utility of p16 expression for distinction of uterine serous carcinomas from endometrial endometrioid and endocervical adenocarcinomas. Immunohistochemical analysis of 201 cases. Am J Surg Pathol. 2009;33:1504–14.
44. Fadare O, Zheng W. Endometrial glandular dysplasia (EmGD):morphological and biologically distinctive putative precursor lesion of Type II endometrial cancers. Diagn Pathol. 2008;3:6.
45. Jarboe EA, Miron A, Monte N, et al. Evidence for a latent precursor (p53 signature) that may precede serous endometrial intraepithelial carcinoma. Mod Pathol. 2009;22:345–50.
46. Silverberg SG, De Giorgi LS. Clear cell carcinoma of the endometrium. Clinical, pathologic, and ultrastructural findings. Cancer. 1973;31:1127–40.
47. Ellenson LH, Ronnett BM, Soslow RA, et al. Endometrial carcinoma. In: Kurman RJ, Ellenson LH, Ronnett BM, editors. Blaustein's pathology of the female genital tract. 7th ed. New York: Springer-Verlag; 2019. p. 473–533.
48. Abeler VM, Vergote IB, Kjorstad KE, et al. Clear cell carcinoma of the endometrium. Prognosis and metastatic pattern. Cancer. 1996;78:1740–7.
49. Fadare O, Stewart CJR. Clear cell carcinoma of the uterine corpus. In: WHO Classification of Tumor Editorial Board, editor. WHO classification of tumor of female reproductive organs. 5th ed. Lyon: IARC Press; 2020. p. 258–9.
50. DeLair DF, Burke KA, Selenica P, et al. The genetic landscape of endometrial clear cell carcinomas. J Pathol. 2017;243:230–41.
51. Ellenson LH, Ronnett BM, Soslow RA, et al. Endometrial carcinoma. In: Kurman RJ, Ellenson LH, Ronnett BM, editors. Blaustein's pathology of the female genital tract. 7th ed. New York: Springer-Verlag; 2019. p. 473–533.
52. Wakui K, Matsui N, Yasuda M, et al. Cytological study of endometrial clear cell carcinoma. Analysis of structural pattern of tumor cells. J Jpn Clin Cytol. 2008;47:269–74. (in Japanese with English abstract).
53. Fadare O, Desouki MM, Gwin K, et al. Frequent expression of Napsin A in clear cell carcinoma of the endometrium: potential diagnostic utility. Am J Surg Pathol. 2014;38:189–96.

54. Lim D, Philip PC, Cheung ANY, et al. Immunohistochemical comparison of ovarian and uterine endometrioid carcinoma, endometrioid carcinoma with clear cell change, and clear cell carcinoma. Am J Surg Pathol. 2015;39:1061–9.
55. Ip PPC, Djordjevic B. Arias-Stella reaction of the uterine corpus. In: WHO Classification of Tumours Editorial Board, editor. WHO Classification of tumor of female reproductive organs. 5th ed. Lyon: IARC Press; 2020. p. 271.
56. Philip PC, Wang SY, Wong OGW, et al. Napsin A, Hepatocyte Nuclear Factor −1-Beta (HNF-1β), Estrogen and Progesteron receptors expression in Arias-Stella raction. Am J Surg Pathol. 2019;43:325–33.